

# Innovated design, simulation and evaluation of potato harvester excavation and separation conveyors

Ibrahim Issa Mohamed Issa<sup>1,3</sup>, Zhaoguo Zhang<sup>1,2,3\*</sup>, Wael El-Kolaly<sup>4,5\*</sup>,  
Faan Wang<sup>2,3</sup>, Yuan Wang<sup>2,3</sup>

- (1. Faculty of Mechanical and Electrical Engineering, Kunming University of Science and Technology, Kunming 650500, China;  
2. Faculty of Modern Agricultural Engineering, Kunming University of Science and Technology, Kunming 650500, China;  
3. Research Center on Mechanization Engineering of Chinese Medicinal Materials in Yunnan Universities, Kunming 650500, China;  
4. Agricultural Engineering Research Institute (AEnRI), Agricultural Research Center (ARC), 256 Dokki, Giza, Egypt;  
5. Solar Energy Research Institute, Yunnan Normal University, Kunming, Yunnan 650500, China)

**Abstract:** To address problems encountered in current potato harvesting machines in hilly and mountainous areas, such as potato damage, poor adaptability, low operational efficiency, and the inability of traditional harvesters to meet the requirements in these areas, a new potato harvester equipped with excavation and a multi-stage separation conveyor was developed by using design and simulation programs as an innovative way to identify the best operating factors. SolidWorks Software was used to design an excavation and a multi-stage separation conveyor. ANSYS Workbench machine static structure analyzed stress, strain, and deformation. The working process of soil and tuber separation was tested and kinematically analyzed by EDEM-RecurDyn and a 5F01M camera. A field experiment was also conducted on the machine under several factors: working speed ( $W$ ), excavation depth ( $D$ ), vibration intensity level ( $V$ ), and conveyor inclination angle ( $N$ ). The quadratic regression orthogonal rotating combination experiment tested four factors with five levels. The results of the non-load experiment showed that the lowest ratio of impurities was at the linear speed level (Q3, S5, O3) for the first and second separation conveyor and the side conveyor, respectively. The results of the field experiment showed that the optimal parameters were the working speed of 1.05 m/s, the digging depth of 180 mm, and the vibration force II inclination angle on the screen surface of 22 degrees, which gave the highest potato lifting rate of 98.8%, and the bruising rate was 1.37%. The damage rate was 1.43%, superior to national industry standards. With its exceptional performance, the machine can effectively meet and solve the challenges of harvesting requirements, making it a valuable tool for the industry.

**Keywords:** potato harvester, multi-stage separation conveyors, agricultural machinery, excavating mechanism

**DOI:** [10.25165/ijabe.20251802.9164](https://doi.org/10.25165/ijabe.20251802.9164)

**Citation:** Issa I I M, Zhang Z G, ElKolaly W, Wang F A, Wang Y. Innovated design, simulation and evaluation of potato harvester excavation and separation conveyors. *Int J Agric & Biol Eng*, 2025; 18(2): 132–145.

## 1 Introduction

Potatoes are the fourth most cultivated crop in the world after rice, wheat, and corn. They are used as food for humans and animals. Potatoes have many advantages, such as rapid growth, high productivity, and high nutritional content<sup>[1,2]</sup>. China designated potatoes as a strategic staple in 2015. China's total potato production and acreage are now among the highest in the world, with an appreciation of developing the country's staple potato strategy and the structural adjustment of the national grain economy<sup>[3-8]</sup>. China is among the top countries in the world in terms

of cultivated area and potato productivity, representing 24% of global production, or 90 million t of fresh potatoes produced annually<sup>[9,10]</sup>.

Although China's potato planting mechanization level is being enhanced yearly, the potato harvesting mechanization level is still low; the potato machine harvesting rate is less than 50%. However, the total mechanization rate of potatoes in the southwest region is only 20.77%<sup>[11-13]</sup>. In comparison, the potato machine yield of hilly and mountainous areas such as Yunnan Province is 4.7%, far lower than the national average level, which has seriously restricted the development of China's potato industry<sup>[14,15]</sup>.

Mechanized harvesting is an essential link in achieving complete mechanization of the potato industry<sup>[16-18]</sup>. Potatoes harvested with combined harvesters have weak skins and high trash content and are not easily stored for long periods, so potato harvesting in China is still mainly done in sections. Developing efficient and low-loss potato harvesting equipment is essential to meet the customary consumption and harvesting methods of potatoes in China.

This study was conducted in Yunnan Province, a region characterized by hilly and mountainous terrain that poses challenges to mechanization. The aim was to address the issues associated with manual potato picking, such as high labor intensity, increased rates of damaged and scratched potatoes, decreased operating efficiency, and low production efficiency. Extensive research has yielded

Received date: 2024-06-18 Accepted date: 2025-02-11

**Biographies:** Ibrahim Issa Mohamed Issa, PhD candidate, research interest: mechanical design, agricultural equipment engineering, Email: [ibrahimeisa14@gmail.com](mailto:ibrahimeisa14@gmail.com); Faan Wang, PhD, research interest: intelligent agricultural machinery, Email: [wfa@kust.edu.cn](mailto:wfa@kust.edu.cn); Yuan Wang, MS candidate, research interest: agricultural equipment, Email: [18838816179@163.com](mailto:18838816179@163.com).

\*Corresponding author: Zhaoguo Zhang, PhD, Professor, research interest: agricultural equipment design and manufacturing. Faculty of Mechanical and Electrical Engineering, Kunming University of Science and Technology, Kunming 650500, China. Tel: +86-15911701001, Email: [zgz@kust.edu.cn](mailto:zgz@kust.edu.cn); Wael El-Kolaly, PhD, research interest: agricultural engineering, greenhouse technology. Agricultural Engineering Research Institute (AEnRI), Agricultural Research Center (ARC), 256 Dokki, Giza, Egypt. Tel: +20-1272967828, Email: [welkolaly2002@gmail.com](mailto:welkolaly2002@gmail.com).

promising results in applying solutions to these problems<sup>[19]</sup>. Elie et al.<sup>[20]</sup> studied the effect of small and medium-sized potato harvesting machines in the hilly and mountainous areas of Yunnan Province on harvest quality, operating efficiency, and damage rate, and the results showed the low ability of these machines to work in those areas<sup>[21,22]</sup>. Wang et al.<sup>[23]</sup> developed a small, tractor-mounted potato harvester that uses a shovel in combination with a conveyor chain for harvesting potatoes, a device for lifting the potato blocks, and a device for collecting the potato blocks for separating the potato soil and collecting the potato blocks. Still, the wounded potato and pollution rates are higher than relevant national industry standards. Researchers<sup>[4,24-26]</sup> added a cylindrical secondary classifier to the small potato harvester to realize potato block picking, grading, and grouping. Still, the number of grading levels does not meet the classification requirements, and the picking efficiency is low.

The second aim of this study was to improve soil-tuber separation, which is critical to the quality of the potato crop. Therefore, it is worth considering how to improve soil separation while reducing damage to the potato tuber<sup>[27]</sup>. The combined harvester can simultaneously complete the tasks of digging, removing soil, collecting, and bagging. However, potato tubers are more likely to be damaged by long contact time with the harvester throughout the combined harvesting process<sup>[28]</sup>. The soil can also be separated in the lifting and haulm removal section. However, the tubers are thrown into the soil after the tuber-soil separation in the digger. The separation time is short, and the requirements for the soil-clearing effect are higher<sup>[29]</sup>. Therefore, separating the tuber-soil mixture dug up by the combine harvester should cause the potato as minor damage as possible. Researchers<sup>[30,31]</sup> studied the effects of a harvester's forward speed and digging depth on potato tuber damage through field tests. Although it is difficult to investigate the process of soil sieving and potato damage, field crop trials are the most direct indicator of post-harvest tuber damage and soil residue<sup>[32-34]</sup>. Court tests do not accurately analyze the process of separating the potato soil mixture; instead, they frequently concentrate on the damage to the potato tubers. Gai et al.<sup>[35]</sup> investigated the impact of droplet treatment on the kinematic features of the screen bar and the damage to potato tubers. Sang et al.<sup>[32]</sup> also examined and analyzed the damage patterns of potatoes upon collision when they fell. They discovered that the distance of the drop when the potato block collides should not be greater than 300 mm, as this increases the risk of deterioration and damage to the potato block, which lowers the potato's market value. Ben et al.<sup>[33]</sup> reported that the variations in the materials of the conveyor belt and the height of the fall exposed potato tubers to skin corrosion. The maximum fall distance for steel parts should be 350 mm, and for rubber parts it should be 500 mm<sup>[34,36]</sup>.

Numerous scientists have studied and analyzed agricultural machinery using the discrete element approach in recent years due to its quick development and the advancement of computer technology. Discrete element approach studies on mechanical harvesting of edible tubers, rhizomes, and root crops are also becoming more common<sup>[37]</sup>. The ANSYS software program was used for virtual assembly, associative design, and finite element analysis to dig a spade for a single-row potato harvester. During harvesting operations, the spade is mainly used for lifting and transporting soil substances, including soil, potato tubers, potato roots, grass, and the separator<sup>[38,39]</sup>.

The available studies report potato harvesters designed for specific conditions in a local area. Integrated between research and production experience, there are currently few models for

mechanized potato harvesting in hilly and mountainous regions of Southern China. Hence, it is necessary to develop machine models that aim to improve the design of structural parameters.

This study developed a new potato harvester to address the problem of potato harvest machines in hilly and mountainous areas in South China. Potato soil excavation and a multi-stage separation conveyor were developed using design and simulation programs as an innovative way to identify the best operating factors. The software was used to design an excavation and a multi-stage separation conveyor. ANSYS Workbench machine static structure analyzed stress, strain, and deformation. The working process of soil and potato tuber separation was tested and kinematically analyzed by EDEM-RecurDyn and a 5F01M camera. A field experiment tested the machine under several factors: working speed ( $W$ ), excavation depth ( $D$ ), vibration intensity level ( $V$ ), and conveyor inclination angle ( $N$ ). The quadratic regression orthogonal rotating combination experiment tested four factors with five levels considering separation effect and potato damage, and the structure and operating parameters of the excavation and separation device were optimized.

## 2 Materials and methods

### 2.1 Experimental site

The study was conducted in March 2023; the prototype was manufactured by Xintianli Agricultural Equipment Manufacturing Company in Yuxi City, Yunnan Province. The no-load test was conducted in Pucao Village, Pingyuan Town, Yanshan County, Wenshan Prefecture, Yunnan Province, and the field harvest test was conducted in September 2023.

### 2.2 Design of potato harvester

According to the agricultural requirements for planting potatoes in the main potato-producing areas of Yunnan Province, the suitable conditions for potato growth and planting are a cultivation layer depth of 120-180 mm and a planting mode of double row per one ridge. The ridge shape parameters are as follows: The height of the ridge is 200-240 mm, the width of the ridge top is 800 mm, the width of the ridge bottom is 900 mm, the spacing between the ridges is 1200 mm, the spacing between the ridges is 300-400 mm, and the spacing between the plants is 280-350 mm. This machine can complete the excavation, transportation, separation, and low-level side laying of single-row and double-row potatoes in one operation. During the operation of the potato harvester, the hydraulic cylinder is used to adjust the angle of the combined digging shovel into the soil. Then, the ridge is broken and excavated. After the lifting multi-stage conveyor separation device separates the potato soil and impurities, they enter the low-level side paving device. This ultimately achieves potato soil separation, transportation, and field paving operations.

The potato harvester was hung behind the tractor and driven by a PTO shaft. The harvester machine harvested potatoes from the field at 900 mm. Table 1 details the main design parameters of the potato harvester, and Figure 1 shows its overall structure.

#### 2.2.1 Design of excavation device

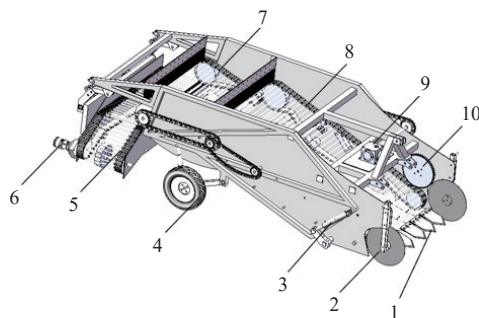
The excavation device is a direct soil contact component whose primary function is to loosen the soil on the ridge, fully excavate the potato soil mixture, and transport it back. The excavation shovel length, width, inclination angle, and depth of penetration all impact the excavation resistance and harvesting effect of the potato block. Among them, the primary function of  $\gamma$  is to ensure the self-cleaning function of the excavation shovel at  $\varphi$  between  $30^\circ$ - $36^\circ$ <sup>[40-42]</sup>, enabling the soil to overcome the overall resistance during

excavation under the sliding cutting effect of the shovel blade and ensuring that the excavated material on the shovel surface can smoothly leave the shovel surface.

$$\gamma < 90^\circ - \varphi \tag{1}$$

**Table 1 Technical parameters of the potato harvester**

Parameter	Value
Overall diameters (length × width × height)/mm	3400×1225×1000
Overall weight/kg	860
Supporting power/kW	36.7-51.5
Number of harvest ridges	1
Working width/mm	900
Adapted ridge width/mm	≤800
Excavation depth/mm	100-260
Pure working time productivity/hm <sup>2</sup> ·h <sup>-1</sup>	0.18-0.32
Center distance between rods at the primary separation screen/mm	52
Center distance between rods at the secondary separation screen/mm	45
Center distance between bars for the side paving separation screen/mm	37
Separation sieve rod diameter/mm	12



1. Digging shovel 2. Cutting disc 3. Hydraulic cylinder 4. Ground wheel 5. Low-side paving device 6. Hydraulic motor 7. Secondary conveying and separating device 8. Primary conveying and separating device 9. Gearbox 10. Crushing plate

Figure 1 Structure diagram of the potato harvester

According to the law of friction, theoretically, the smaller inclination angle of the shovel blade increases the ability to cut soil and grass. However, if the value is too small, it will reduce the wear resistance with an increase in potato damage and leakage rate. This design takes  $\gamma_1=46.8^\circ$ , six single shovels are symmetrically distributed along the installation horizontal axis, and the three shovels correspond to the single ridge surface. The angle between the two adjacent shovels is paired  $\gamma_2$  at  $93.6^\circ$ , conducive to the cutting, crushing, and drag reduction of dense soil, as shown in Figure 2.

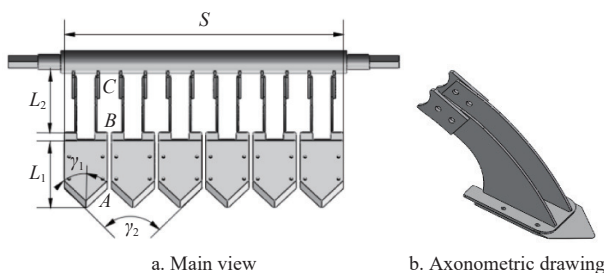


Figure 2 Diagram of the excavating device structure

The excavation shovel width is mainly related to the underground distribution of potato tubers, row spacing, plant spacing, growth direction, and deviation in the walking route of

machinery<sup>[43-46]</sup>. The effective working width  $S$  of the excavation device should be slightly more significant than the width of the ridge bottom. The calculation formula for the working width of the potato harvester's excavation shovel is

$$S = M + b + 3\varepsilon + 2c \tag{2}$$

$$\varepsilon = \sqrt{\varepsilon_M^2 + \varepsilon_b^2} \tag{3}$$

where,  $c$  is taken as 50-80 mm.

Based on the agronomic requirement of a ridge bottom width of 900 mm, the practical working width  $S$  of the excavation shovel group is 946 mm.

The structural diagram of the excavation device is shown in Figure 2. The excavation device consists of two sections: the shovel body and the soil-crushing plate. The excavation device is divided into the front section length  $L_1$  and the rear section length  $L_2$ , with  $L_1$  determined by the inclination angle of the shovel surface  $\delta$  ( $15^\circ$ ) and the average excavation depth  $h_1$  (140-180 mm). The calculation equation is

$$L_1 = \frac{h_1}{\sin\delta} \tag{4}$$

The law of energy conservation determines the length  $L_2$  of the rear section of the excavation device. The excavated shovel moves along the shovel surface at the machine's forward speed to point  $B$  and continues to rise along the shovel surface to the end at point  $C$ . When the speed is zero, the soil begins to expand and loosen, scattering towards both sides of the shovel in a pile-like manner. Potato tubers gradually appear on the shovel surface as the soil falls off. The potato soil mixture's kinetic energy (point  $B$ ) is used to overcome the friction work  $W_f$  of the excavation shovel  $AC$  section and the gravitational potential energy  $W_G$  of the mixture rising.

$$W_f = Rt_w g \varphi L_2 = mgL_2 t_w g \varphi \cos \delta \tag{5}$$

$$W_G = mgh_2 = mgL_2 \sin \delta \tag{6}$$

The energy conservation equation for the potato soil mixture passing through the  $BC$  segment is

$$\frac{mv_w^2}{2} = mgL_2 t g \varphi \cos \alpha + mgL_2 \sin \delta \tag{7}$$

$$L_2 = \frac{v_w^2 \cos \delta}{2g \sin(\delta + \varphi)} \tag{8}$$

The total length is

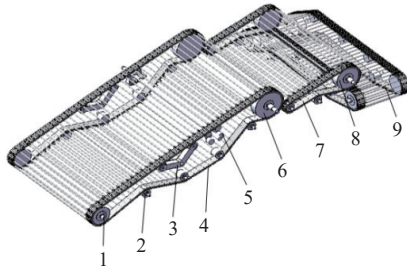
$$L = L_1 + L_2 = \frac{h_1}{\sin \delta} + \frac{v_w^2 \cos \delta}{2g \sin(\gamma + \varphi)} \tag{9}$$

A soil plow crushing plate is installed after the excavation shovel to reduce soil blockage effectively. The soil- potato mixture is split, sheared, and bent on the crushing plate<sup>[43,47]</sup>, enabling the potato soil mixture to be effectively transported to the separation device, making the separation more complete, reducing the power consumption of vibration separation, and achieving a better potato soil separation effect.

### 2.2.2 Design of lifting conveyor multi-stage device

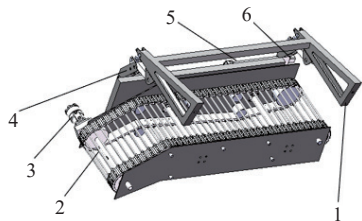
The design of the lifting conveyor multi-level conveying separation device parts is shown in Figure 3. The multi-stage transportation and separation device adopts a three-stage potato soil separation process structure. The primary lifting conveyor has a length of 1600 mm with an installation angle of  $22^\circ$ <sup>[8,10,47,48]</sup>. The length of the secondary lifting conveyor is designed to be 900 mm, and the lateral conveying dimension is 1300 mm×600 mm; that's

too low laying at the end of the falling potato to minimize the height of the potato drop with the inclined angle of the falling potato end is 45°, as shown in Figure 4. The center distance of the primary lifting conveyor rods is designed to be 52 mm, the center distance of the second-level lifting conveyor rods is 45 mm, and the center distance of the lateral conveying rods is 37 mm.



1. Guide wheel 2. Tension wheel 3. Passive vibration device 4. Primary conveying separation lifting conveyor 5. Active vibration device 6. Primary conveying driving wheel 7. Secondary conveying separation lifting conveyor 8. Secondary conveying driving wheel 9. Side conveyor

Figure 3 Structure diagram of conveying and separating device



1. Linkage support 2. Lifting conveyor 3. Hydraulic motor 4. Ball head telescopic adjusting rod 5. Optical axis and adjustment track 6. Adjusting rocker

Figure 4 Structure diagram of a low-side paving device

The vibration separation effect of the separation lifting conveyor is mainly achieved by the active and passive vibration devices installed below the right side of the primary conveying separation device, as shown in Figures 5 and 6.

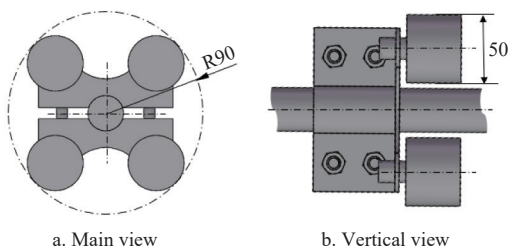


Figure 5 Structure diagram of an active vibration device



1. Tensioning wheel 2. Passive vibration device 3. Primary main vibration device 4. Primary lifting conveyor 5. Collecting plate 6. Supporting wheel 7. Primary driving wheel 8. Cushion curtain

Figure 6 Structure of vibration conveying separation part

### 2.3 Analysis of excavation and separation devices

Theoretical analysis can explain the excavation mechanism and

the potato soil mixture’s movement characteristics well. Still, obtaining the phenomenon of intuitive movement is necessary to compensate for the lack of theoretical analysis. The kinematic analysis of potato block throwing stages gave the conveying and separation devices the optimal speed. The analysis of these devices can explain the parameters that affect potato damage. The analyses and design parameters of the excavation and separation devices meet the harvesting requirements.

#### 2.3.1 Analysis of excavation device

The ANSYS workbench software program was used to analyze each component as structural steel material, so the selected component was divided into meshes chosen according to the force surface of all component surfaces. Therefore, the number of cells and nodes should be significantly increased. With both sides of each component, the number of discrete elements for meshing was 7850, with a yield strength of 250 MPa, a Poisson’s ratio of 0.3, and a Young’s modulus of 25 000 MPa. After completing the material selection, the connections between each component were selected in ANSYS based on the actual relationship between the models of the excavator assembly; each shovel body assembly was fixed by bolts or welding without any movable joints, and the relationship between the components was simplified to a fixed relationship during the analysis process. Therefore, when setting the relationship, it was selected to be bonded and firmly connected. Then, the shovel body assembly was meshed using a tetrahedral mesh division, as shown in Figure 7.

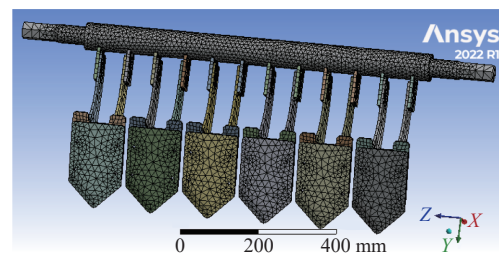


Figure 7 Mesh generation

Analyzing the shovel body assembly reveals six excavation shovels, each with a force of 737 N. After applying the load to each excavator, the overall constraint and force load of the excavator assembly are shown in Figure 8.

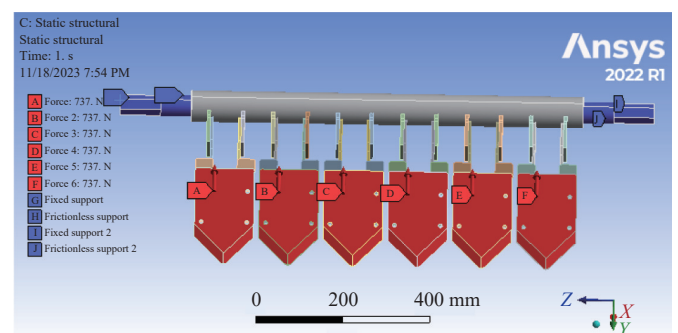


Figure 8 Excavation shovel assembly constraints and force loads

The diameter of the connection part between the excavator shaft and the excavator support was designed to be 72 mm. In comparison, the diameter of the shoulder that matches the flange shaft sleeve was designed to be 48 mm. The middle pipe fittings used a steel pipe with a diameter of 72 mm and a wall thickness of 10 mm as the raw material. After modifying the model, grid division, total deformation, strain, and stress loads were performed and solved. Then, the figure was drawn, as shown in Figure 9.

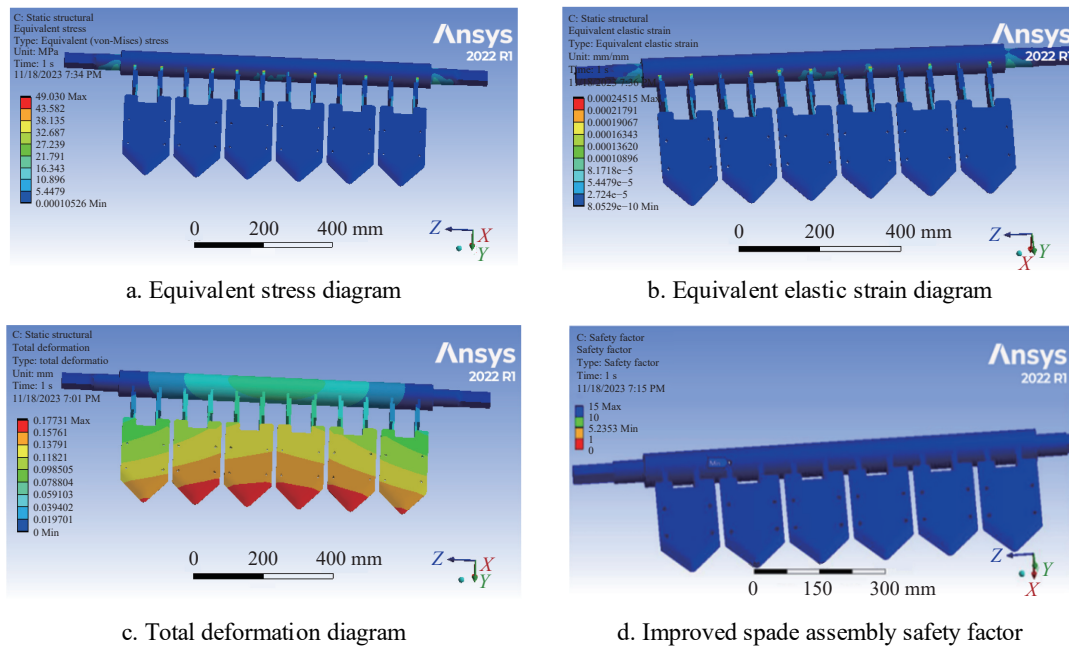


Figure 9 Excavation device analyses

After the above improvement, the maximum stress value of the graph is 49.03 MPa, the maximum strain value is  $2 \times 10^{-4}$  mm, and the maximum deformation is 0.177 mm. It can be concluded that the area with high stress is at the welding position between the shaft and the pipe fitting, with a value of 30-40 MPa, as shown in Figure 9d. This stress value does not exceed the allowable stress value of the material. The maximum deformation of the improved shovel body also occurs in the range of the shovel tip from the 3<sup>rd</sup> to 4<sup>th</sup> excavation shovel on the left, with a deformation of 0.26-0.29 mm, an increase of 0.03 mm compared to the deformation before the improvement. The deformation of the shovel shaft is an elliptical shape that spreads from the middle to the outside, with a maximum deformation of 0.01 mm. To further verify the structural reliability of the mechanism, the safety coefficient of the mechanism was calculated. The safety factor of its entire machine is mostly above 10.0, and the safety factor of sharp corner positions such as shaft shoulder, excavator support, and shaft tube welding is 1.0, which is greater than the design standard of ordinary machinery.

### 2.3.2 Analysis of the movement characteristics of potato soil mixture

When the angle between the separating lifting conveyor surface and the forward direction of the harvester is greater than the internal friction angle of the potato soil mixture, the potato block generates a “backflow” phenomenon, which increases the dynamic damage, squeezing friction and fatigue accumulation damage of the potato during transportation and separation. The potato soil mixture entering the primary conveying and separation device will undergo complex processes such as conveying, separation, scattering, and jumping. Under the action of the vibration device, the potato soil mixture changes from “non-vibration inclined flat conveying” to “vibration inclined folded line conveying”, and its stress state changes. The transportation and separation process of the potato soil mixture is accompanied by alternating changes in two motion states, the separation effect of the potato soil mixture and the quality of potato harvest.

The motion characteristics of the potato soil mixture in the vibration-free stage of the primary and second conveyors separation are similar. Taking the force analysis of the potato soil mixture in the vibration-free stage of the primary conveyor separation as an

example, at this time, the roller of the vibration device does not contact the conveyor, and the conveyor is in an inclined and flat conveying state. The force analysis is shown in Figure 10. The force state of the potato block on the conveyor is approximately regarded as a rigid body, which includes the gravity of the potato soil mixture itself, the reaction force  $F_{N1}$  on the sieve surface, the frictional force generated by the relative motion between the conveying separation and conveyor and the potato soil mixture along the sieve surface, and the inertial force of the potato soil mixture itself. Ignoring the micro-excitation effect of the separation screen on the potato soil mixture and the force between the potato soil mixture and the vine debris, the dynamic equation for the movement of the potato soil mixture along the transport separation screen is obtained as follows:

$$F_{s1} - F_{g1} - m_1g \sin \alpha_1 = ma \tag{10}$$

where,  $F_{s1}$  is the frictional force between the conveying separation and the potato soil mixture, N;  $F_{g1}$  is the inertia force of the potato soil mixture itself, N;  $\alpha_1$  is the angle between the conveyor separation and the horizontal plane, ( $^\circ$ );  $a$  is the acceleration of the upward movement of the potato soil mixture along the sieve surface,  $m/s^2$ .

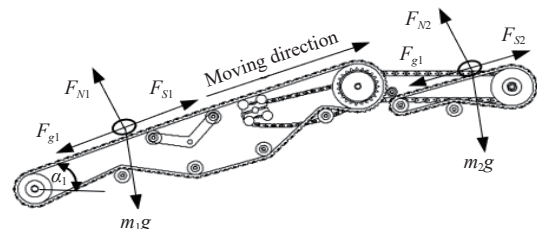


Figure 10 Analysis of the stress of the potato soil mixture in the inclined flat conveying section

According to the principle that the motion of the conveying separation can be approximated as a “simple harmonic motion”<sup>[49]</sup>, when the potato soil mixture moves to the vibrating inclined harvested line conveying section, the conveying separation is lifted by the active vibration device, and when the vibration reaches its maximum amplitude, the potato soil mixture will be scattered and jump. The force analysis of the critical point for the dispersal jump of the potato soil mixture is shown in Figure 11. Before the

dispersal jump, the forces on the potato soil mixture include the gravity of the potato soil mixture itself, the reaction force  $F_{N3}$  on the sieve surface, the frictional force  $F_{s3}$  generated by the relative motion between the conveying separation and the potato soil mixture along the sieve surface, and the inertial force  $F_{g3}$  perpendicular to the sieve surface that the potato soil mixture is subjected to. A Cartesian coordinate system is established, with the  $x_2$  axis parallel to the velocity direction of the conveyor separation screen line and the  $y_2$  axis perpendicular to the conveyor direction upward. When the potato soil mixture disperses and jumps, it is subjected to a support reaction force  $F_{N3}=0$ . At this time, an equilibrium equation is established along the  $y_2$  axis:

$$F_{g3} \gg m_3 g \cos \alpha_2 \quad (11)$$

$$F_{g3} = -m_3 \alpha_2 \quad (12)$$

where,  $\alpha_2$  is the working inclination angle of the conveyor separation, ( $^\circ$ ).

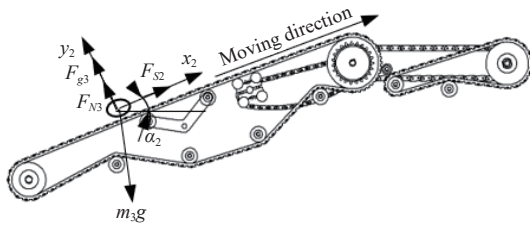
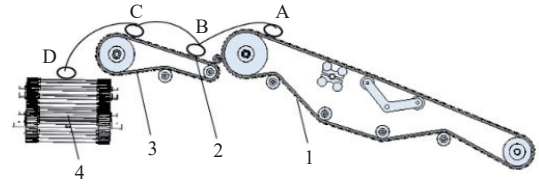


Figure 11 Force analysis of potato soil mixture in the process of throwing and jumping

When the vibration amplitude is high, it causes the potato soil mixture to scatter and jump, making it suitable for harvesting conditions where the soil is relatively sticky and firm. If there is no vibration or the vibration amplitude is small, it is ideal for harvesting conditions in sandy soil. However, if the vibration amplitude is too large, it can easily cause damage to the potato and skin and even lead to the phenomenon of “backflow” of potato blocks. During the potato harvesting process, factors such as the physical characteristics of the potato variety, soil type, harvesting speed, and lifting conveyor speed should be comprehensively considered<sup>[4]</sup>. This study adopts a “high-frequency, low-amplitude” lifting conveyor vibration form to separate the potato soil and reduce damage. In the case of low vibration amplitude, designing an active vibration device with four rollers increases the number of times the roller contacts the sieve surface per unit time, further increasing the vibration frequency of the lifting conveyor.

### 2.3.3 Kinematic analysis of potato block throwing stage

The dropping stage of the potato block mainly refers to the potato block falling from the end of the primary conveying separation device into the secondary conveying separation device, from the end of the secondary conveying separation device into the low-level side paving device, and the potato block falling from the end of the side conveyor into the ground. Therefore, the secondary conveying separation and the side conveyor rod are wrapped in soft rubber to reduce the damage caused by the potato block falling. The movement process of the potato block is shown in Figure 12. The damage to the potato block mainly occurs in the collision between the end of the primary conveyor separation and the second conveyor separation rod ( $A \rightarrow B$  process), the collision between the end of the second conveyor separation and the side conveyor rod ( $C \rightarrow D$  process), and the collision damage between the end of the side conveyor and the ground.



1. Primary conveying separator 2. Potato block 3. Secondary conveying separator 4. Side conveyor

Figure 12 Schematic diagram of the potato movement process

The potato block falls into the surface stage from the low side paving device, with a low height of falling, and the surface soil is relatively loose after harvesting, resulting in less damage to the potato block. The motion characteristics of the potato block falling from the primary conveyor to the secondary conveyor are similar to the motion characteristics of the secondary conveyor falling into the side conveyor, and the process of the secondary conveyor separation screen falling into the side conveyor needs to consider the horizontal displacement to prevent the potato block from flying out and colliding with the side conveyor device, causing secondary damage to the potato or falling onto the surface behind the machine. Therefore, this study takes the motion characteristics of potato blocks falling into the side conveyor through the secondary conveyor as an example for analysis (Figure 13).

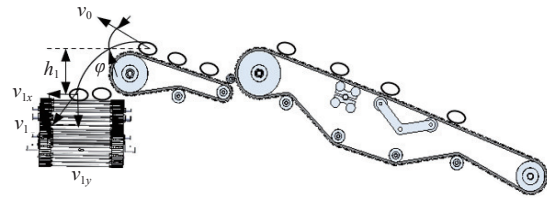


Figure 13 Motion analysis of potato throwing at the end of two-stage conveying separation screen

When the potato block moves to the end of the secondary conveyor, due to a certain angle between the conveyor and the horizontal plane, the speed direction of the potato block being thrown out is the same as the linear speed direction of the conveyor separation. Ignoring the impact of possible collisions, friction, and air resistance between soil and potato, the potato block is thrown out. It moves at a uniform speed in the horizontal direction. In contrast, the vertical direction is first decelerated to the highest point. Afterward, a uniform acceleration motion is performed vertically to the surface of the side conveyor. According to the law of energy conservation, the maximum elevation after throwing is:

$$\frac{1}{2} m_4 v_0^2 \sin^2 \varphi = m_4 g h_0 \quad (13)$$

$$h_0 = \frac{v_0^2 \sin^2 \varphi}{2g} \quad (14)$$

where,  $m_4$  is the mass of the potato block, kg;  $v_0$  is the linear velocity at the end of the secondary conveyor separation for the potato block being thrown out, m/s;  $\varphi$  is the angle between the conveyor and the horizontal plane of the secondary conveying, ( $^\circ$ );  $h_0$  is the maximum height to which the potato block rises after being thrown out, mm.

The linear velocity of the secondary conveyor separation is directly proportional to the speed of the potato block being thrown out. Suppose the speed of the potato block being thrown out is too high. In that case, the displacement of the potato block in the vertical direction will be more significant, the time it takes for the

potato block to fall will be longer, and the horizontal uniform motion displacement will be more critical. If the horizontal displacement is too high, it will cause the potato block to collide with the output device on the side and cause secondary damage to the potato, or fall onto the surface behind the implement, affecting the quality and efficiency of harvest. Taking the maximum linear velocity  $v_0$  of the secondary conveyor separation as 2.25 m/s and substituting it into Equation (14), the maximum lifting height  $h_0$  after the potato block is thrown out is 3 mm. The movement of the potato block in the horizontal direction after being thrown out is divided into two stages: the stage of vertical uniform deceleration movement to the highest point, and the stage of uniform acceleration movement from the highest point to the side conveyor.

$$h_0 + h_v = \frac{1}{2}gt^2 \quad (15)$$

$$x = tv_0 \cos \varphi \quad (16)$$

where,  $h_v$  is the vertical height of the side conveyor when the potato block is thrown off the end of the secondary conveyor separation and falls, mm;  $t$  is the time for the potato block to fall off the end of the secondary conveyor and onto the side conveyor, s;  $x$  is the horizontal displacement of the potato block after being thrown away, mm.

According to simultaneous Equations (15) and (16), when the potato block is thrown away from the end of the secondary conveyor and drops to the vertical height  $h_1$  of the side conveyor, it is designed to be 200 mm. By substituting the data, it is calculated that the horizontal displacement of the potato after being thrown away is 430 mm. The designed side output device has a conveyor width of 460 mm, a gap of 40 mm between the conveyor and the two guard plates, and an actual working width of 500 mm, meeting the harvesting requirements under the maximum throwing speed of the potato block. During the actual harvesting process, due to the friction and collision of factors such as potato and potato soil and the influence of air resistance, the actual throwing speed of the potato block is less than the calculated maximum throwing speed. Furthermore, experiments have proven that the optimal speed of the secondary conveying and separation device is not the maximum linear speed. The potato block did not collide with the side conveyor device, so there was no secondary damage to the potato and it did not fall onto the surface behind the machine. The design parameters of the low-level side paving device meet the harvesting requirements.

After the potato block is thrown away and rises to the maximum height, it undergoes a free-fall motion in the vertical direction. Based on the above derivation, the vertical velocity when the potato block collides with the side conveyor rod can be calculated:

$$v_{1y} = \frac{\sqrt{2g(h_0 + h_v)}}{g} \quad (17)$$

If the potato block moves uniformly in a straight line in the horizontal direction, the horizontal velocity when the potato block collides with the side conveyor rod is:

$$v_{1x} = v_0 \cos \varphi \quad (18)$$

The collision speed when the potato block falls onto the side conveyor is:

$$v_1 = \sqrt{v_{1x}^2 + v_{1y}^2} \quad (19)$$

where,  $v_{1y}$  is the vertical velocity at the moment of collision between the potato block and the side conveyor, m/s;  $v_{1x}$  is the

horizontal velocity at the moment of collision between the potato block and the side conveyor, m/s;  $v_1$  is the collision velocity between the potato block and the side conveyor, m/s.

Equations (17) to (19) can be used to calculate the maximum collision velocity as 2.12 m/s by substituting the data. However, due to the potato soil mixture's friction, compression, collision, and air resistance, the collision velocity should be smaller than the theoretical maximum collision velocity, thus meeting the design requirements.

#### 2.3.4 Simulation model of the separation process based on RecurDyn-EDEM

Based on EDEM-RecurDyn, the simulation model for the separation conveyor device was established to study the motion of potato tubers on the separation conveyor. A virtual simulation environment was created with a 0.2 m cubic box positioned at the front end of a lifting chain. Gravity was defined along the Y-direction with an acceleration of 0.98 m/s<sup>2</sup>. Inside the box, a discrete element model of potato tubers was generated, combined with a specific proportion of soil particles to replicate the potato soil complex in a separation conveyor operation. The simulation parameters were set to a duration of 4 s with a step size of 0.01 s (see Figure 14).

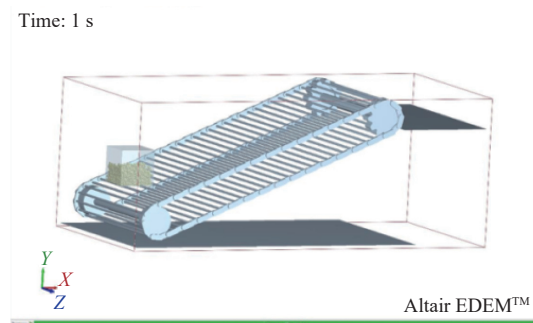


Figure 14 Establishment of the coupling simulation environment

Tuber-soil separation of the potato soil complex was mainly completed in 2.0 s. During this time, at a lifting speed of 1.42 m/s and an inclination of 22°, the lifting chain's vibration separated the tubers from the soil. Fine soil particles leaked through bar gaps while friction moved the potato soil complex upward. Soil detachment increased separation efficiency (Figure 15).

#### 2.4 No-load experimental design and treatments

According to theoretical analysis, the conveyor's operating speed impacts the sliding form, separation effect, and adequate coverage area of the potato soil mixture on the conveyor. To determine the sliding mode and material distribution between the potato block (soil block) and the conveyor, the optimal working parameter combination for the operating speed of the tertiary conveyor separation is determined, and the optimal speed parameter combination is used as the field operation parameter. The experiment was arranged using the quadratic rotation orthogonal combination experimental design method, with the linear velocity of the primary conveyor separation ( $Q$ ): ( $Q_1=0.44$ ,  $Q_2=0.84$ ,  $Q_3=1.42$ ,  $Q_4=2$ ,  $Q_5=2.4$  m/s), the linear velocity of the secondary conveyor separation ( $S$ ): ( $S_1=0.6$ ,  $S_2=0.92$ ,  $S_3=1.4$ ,  $S_4=1.88$ ,  $S_5=2.2$  m/s), and the lateral output linear velocity ( $O$ ): ( $O_1=0.4$ ,  $O_2=0.64$ ,  $O_3=1$ ,  $O_4=1.36$ ,  $O_5=1.6$  m/s) as the experimental factors. Using impurity content and soil coverage as experimental indicators, high-speed image data of the changes in the position and posture of the conveyor separation under various factors were collected, as well as the corresponding movement of soil blocks relative to the conveyor

separation. The machine selected in the experiment had a lower forward speed than regular operation, mainly because the lower forward speed of the machine can reduce the amount of material falling onto the conveyor separation, facilitating effective capture of the motion images of potatoes relative to the conveyor separation. The conveyor separation line speed can be adjusted by controlling the tractor throttle to change the power output shaft speed, combined with the gearbox. The linear speed of the side conveyor device was adjusted by adjusting the hydraulic adjustment device. The camera was fixed onto the harvester frame with a bracket and tilt, and the camera height was changed to capture the distribution of soil blocks on the entire conveyor separation at a certain angle, as shown in Figure 16. During the experiment, the high-speed camera was kept waiting for recording. After the tractor started running smoothly, the high-speed camera began to record the distribution of soil blocks on the conveyor separation. Based on the relative motion

characteristics of the potato conveyor separation and the changes in the coverage of the potato soil mixture, the mechanism by which the conveyor separation parameters affect the performance of the conveyor separation was analyzed.

Soil from a 10 m stable testing area was randomly collected for testing, data was recorded, and one test was completed by analyzing the significance of the factors that affect the experimental indicators through the experimental results. A more suitable combination of various factors is ultimately obtained based on actual needs. Other testing equipment included tractor Dongfanghong 704, Qianyanlang 5F01M high-speed camera produced by Hefei Fuhuang Junda High Tech Information Technology Co., Ltd., Vite BWT901CL intelligent attitude sensor, XCC 988 electronic scale, Qike QC advanced steel tape measure, meter ruler, soil firmness meter, and soil moisture meter produced by Zhejiang Topp Company.

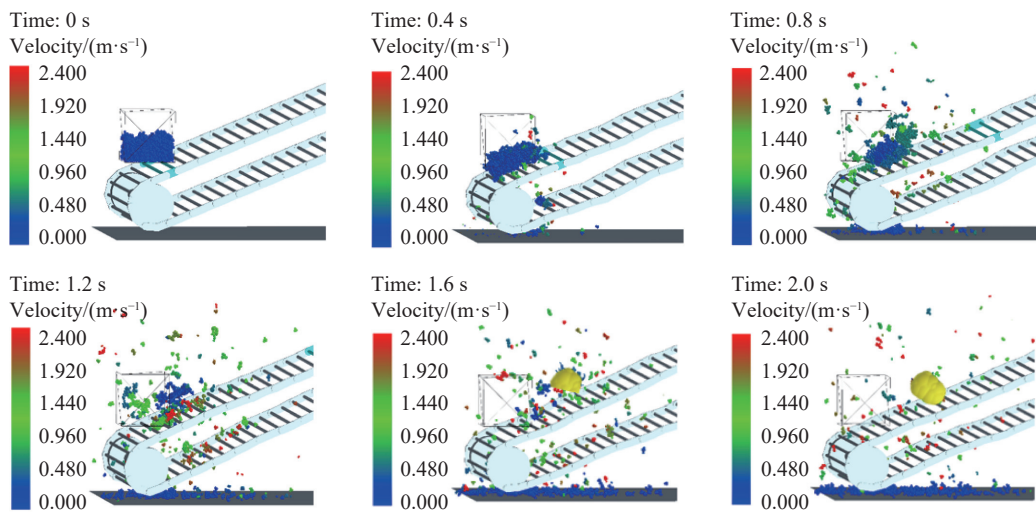


Figure 15 Movement trajectory of the potato tuber



Figure 16 Bench test and high-speed photography layout plan

Except for the three factors mentioned above, other factors were set to remain unchanged, and experimental data statistics and analysis were completed according to the experimental requirements. The experimental results are listed in Table 3. The impurity content refers to the percentage by mass of impurities, including crushed soil, output by the low-level side paving device after a complete test, drawing on the concept of vegetation coverage in ecology<sup>[50,51]</sup>. The soil coverage on the conveyor is defined as the percentage of the vertical projection area of the soil on the separation sieve surface relative to the total area of the high-speed photography to continuously vertically capture images of the distribution status of soil on the sieve surface. After the experiment

was completed, Matlab was used to interpret the number of pixels in the selected image range, read and calculate the number of pixels  $w$  in the histogram, and calculate the soil coverage on the separation sieve using Equation (20):

$$\eta = \frac{\sum_{i=1}^n w_i}{w} \times 100 \tag{20}$$

where,  $\eta$  is the soil coverage on the separation sieve, %;  $w_i$  is the number of pixels in the  $i$ -soil block;  $w$  is the number of pixels in the conveyor separation image.

### 2.5 Field experimental design and treatments

The tractor Dongfanghong 704 was selected for the field experiment, maintaining a linear speed of 1.42 m/s for the primary conveyor separation, 2.2 m/s for the secondary conveyor separation, and 1.0 m/s for the side conveyor. According to the national industry standard NY/T 648-2015 “Technical Specification for Quality Evaluation of Potato Harvester”, the field experiment was conducted to determine the harvesting performance of the potato harvester under sticky and heavy soil conditions, considering the main factors that affect its harvesting effect<sup>[20,36]</sup>. Through theoretical analysis and calculation, it can be concluded that the vibration intensity of the conveyor separation and the inclination angle of the conveyor are the main factors affecting the separation and crushing effect. Therefore, under the conditions of determining the optimal speed of the conveyor separation in the no-load test, to verify the

performance of the excavator and the separation effect of the conveyor separation, an orthogonal test method with a total of 25 mixed experiments was designed using the standard design sheet L25 (5<sup>4</sup>). Each experiment area was 31.5 m<sup>2</sup> (35 m×0.9 m), separated by a distance of 1 m between each experiment and by a distance of 10 m at the end of each experiment (see Figure 17).

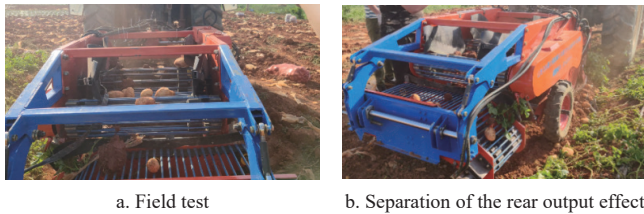


Figure 17 Field harvest experimental test

Based on the analyses of the main factors in previous studies, four factors and five levels are presented in Table 2, including the working speed (*W*), excavation depth (*D*), vibration intensity level (*V*), and conveyor inclination angle (*N*).

Table 2 Factors and levels for the orthogonal test

Level	Factors			
	Working speed <i>W</i> /m·s <sup>-1</sup>	Excavation depth <i>D</i> /mm	Vibration intensity <i>V</i>	Inclination angle <i>N</i> /(°)
1	0.75	120	I	7
2	0.83	140	II	11
3	0.94	160	III	15
4	1.05	180	IV	19
5	1.16	200	V	22

### 2.6 Performance evaluation

#### 2.6.1 Potato lifting percentage

The potato lifting percentage was calculated to ascertain the mass of the potato which remained unharvested. It was defined as follows:

$$Lift \% = \frac{W_1}{W_1 + W_2} \times 100 \quad (21)$$

where, *W*<sub>1</sub> is the total mass of harvested potato, kg; *W*<sub>2</sub> is the total mass of unharvested potato, kg.

#### 2.6.2 Potato damage percentage

After the potatoes were harvested by machine, they were categorized into two groups: reasonable and damaged. The weight of each tuber group was measured individually. The total damage percentage of the potato can be obtained from the following equation:

$$Damage \% = \frac{W_4}{W_3 + W_4} \times 100 \quad (22)$$

where, *W*<sub>3</sub> is the total mass of good potato, kg; *W*<sub>4</sub> is the total mass of potato damaged by the potato harvester, kg.

#### 2.6.3 Potato bruising percentage

Potatoes were bruised either by striking with soil clods or due to the rubbing action while being conveyed by multi-stage conveyors. Bruised potatoes are defined as follows:

$$Bruised\ potato \% = \frac{W_4}{W_5 + W_4} \times 100 \quad (23)$$

where, *W*<sub>5</sub> is the total mass of bruised potatoes, kg.

## 3 Results and discussion

### 3.1 Effect of multi-stage conveyor speed on impurity content and soil coverage

The results of the multi-stage conveyor speed test are shown in Table 3. The multiple regression and the fitting analysis were performed by Design Expert 8.0.6 software (Stat-Ease Inc., Minneapolis, MN, USA); the various regression equations for impurity content *Y*<sub>1</sub> and soil coverage *Y*<sub>2</sub> are shown in Equations (24) and (25).

$$Y_1 = 5.29 + 0.34Q - 0.98S + 0.36QO - 0.46SO - 0.41Q^2 \quad (24)$$

$$Y_2 = 70.29 + 7.61Q - 8.69Q^2 + 0.62S^2 \quad (25)$$

Table 3 Experimental scheme and results

Serial No.	Factor			Impurity content <i>Y</i> <sub>1</sub> /%	Soil coverage <i>Y</i> <sub>2</sub> /%
	<i>Q</i> /ms <sup>-1</sup>	<i>S</i> /ms <sup>-1</sup>	<i>O</i> /m·s <sup>-1</sup>		
1	Q1	S3	O3	3.46	74.98
2	Q2	S2	O2	5.24	70.28
3	Q2	S4	O2	3.26	68.91
4	Q2	S2	O4	3.92	71.23
5	Q2	S4	O4	3.12	70.92
6	Q3	S3	O1	3.45	65.17
7	Q3	S1	O3	4.29	66.56
8	Q3	S3	O3	3.28	60.86
9	Q3	S3	O3	3.49	68.12
10	Q3	S3	O3	3.45	65.93
11	Q3	S3	O3	3.48	66.31
12	Q3	S3	O3	3.41	63.27
13	Q3	S3	O3	3.28	64.14
14	Q3	S3	O3	3.51	67.77
15	Q3	S3	O3	3.47	62.84
16	Q3	S3	O3	3.38	63.21
17	Q3	S5	O3	2.58	68.96
18	Q3	S3	O5	3.63	61.25
19	Q4	S2	O2	3.81	53.29
20	Q4	S4	O2	2.61	51.86
21	Q4	S2	O4	3.87	52.19
22	Q4	S4	O4	2.86	50.64
23	Q5	S3	O3	2.68	38.67

For impurity content and soil coverage, ANOVA was performed separately, and the results are listed in Table 4. The influence of *Q* and *S* on impurity content *Y*<sub>1</sub> was highly significant (*p*<0.01). The interaction between *Q* and *O*, as well as the interaction between *S* and *O*, had a substantial impact on the impurity content *Y*<sub>1</sub> (0.01<*p*<0.05). The quadratic term of the linear velocity *Q* of the primary conveyor separation had a significant impact on the impurity content *Y*<sub>1</sub> (0.05<*p*<0.1). The influence of other factors on the impurity content *Y*<sub>1</sub> of the experimental indicator was not significant (*p*>0.1). The quadratic terms of *Q* and *Q* had a substantial impact on soil coverage *Y*<sub>2</sub> (*p*<0.01). The quadratic term of *S* had a significant impact on soil coverage *Y*<sub>2</sub> (0.01<*p*<0.05). The impact of other factors on the experimental indicator soil coverage *Y*<sub>2</sub> was not significant (*p*>0.1).

From the analysis results, *Q*, *S*, and *O* in the primary term significantly affected the impurity content *Y*<sub>1</sub> and soil coverage *Y*<sub>2</sub>. *QO* and *SO* significantly influenced the impurity content *Y*<sub>1</sub> in the interaction term. In the secondary term, *Q*<sup>2</sup> significantly affected the impurity content *Y*<sub>1</sub>. There were no interaction or quadratic terms for the soil coverage rate, as it conformed to the linear model. The effects of the interaction terms on the impurity content *Y*<sub>1</sub> are shown in Figure 18.

As shown in Figure 18, when the linear velocity of the secondary conveyor separation is constant, the impurity content *Y*<sub>1</sub>

shows a gradually decreasing trend as the linear velocity of the primary conveyor separation increases. The optimal linear velocity range of the primary conveyor separation is 1.42-2.40 m/s. When the linear velocity of the primary conveyor separation is constant, the impurity content  $Y_1$  is generally positively correlated with the linear velocity of the secondary conveyor separation. The optimal range of the linear velocity of the secondary conveyor separation is 1.4-2.2 m/s. Among these, the linear velocity of the primary conveyor separation is the main factor affecting the impurity

content. The optimal operating parameters for the conveyor separation are the linear velocity of 1.42 m/s for the primary, 2.2 m/s for the secondary, and 1 m/s for the side conveyor line. Under these operating parameters, the impurity content is 2.56%, and the soil coverage on the conveyor is 69.11%. Under no-load conditions, the soil coverage is approximated as the distribution of material sieve cover during field operations. The changes in posture and the effects of high-speed photography are shown in Figures 19 and 20.

**Table 4 Variance analysis**

Source of variation	Trash content					Soil coverage				
	Sum of squares	Freedom	Mean square	$F$	$p$	Sum of squares	Freedom	Mean square	$F$	$p$
Model	6.31	9	0.70	10.71	0.0001***	1531.21	9	170.13	39.66	< 0.0001***
$Q$	0.56	1	0.56	8.58	0.0017***	1062.93	1	1062.93	247.75	< 0.0001***
$S$	3.65	1	3.65	55.78	< 0.0001***	3.96	1	3.96	0.92	0.3544
$O$	0.01	1	0.01	0.20	0.0043	4.57	1	4.57	1.06	0.3211
$QS$	0.05	1	0.05	0.83	0.3797	4.09	1	4.09	0.95	0.3466
$QO$	0.40	1	0.40	6.12	0.0279**	2.29	1	2.29	0.53	0.4780
$SO$	0.36	1	0.36	5.54	0.0350**	1.07	1	1.07	0.25	0.6266
$Q^2$	0.26	1	0.26	3.96	0.0679*	124.64	1	124.64	29.05	0.0001***
$S^2$	0.07	1	0.07	1.00	0.3355	19.16	1	19.16	4.47	0.0445**
$O^2$	0.02	1	0.02	0.29	0.5990	5.61	1	5.61	1.31	0.2735
Residual	0.85	13	0.07			55.77	13	4.29		
Lack of fit	0.79	5	0.16	20.79	0.0002	7.77	5	1.55	0.26	0.9235
Error	0.06	8	0.01			48.01	8	6.00		
Sum	7.16	22				1586.98	22			

Note: \* indicates significant impact ( $0.05 < p < 0.1$ ), \*\* indicates significant impact ( $0.01 < p < 0.05$ ), and \*\*\* indicates extremely significant impact ( $p < 0.01$ ).

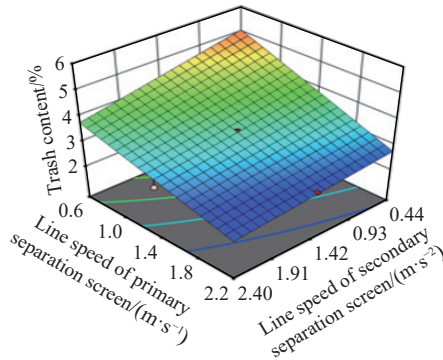


Figure 18 Response surface of impurity rate

It can be obtained from the three-axis attitude changes by taking the forward direction of the machine as the negative  $x$ -axis direction. Under the optimal conveyor separation working parameters, the working attitude of the  $y$ -axis and  $z$ -axis directions of the conveyor separation is greatly affected by the excitation during machine operation, while the  $x$ -axis is less excited. The

fluctuation of the  $x$ -axis acceleration amplitude can be ignored compared to the changes on the  $y$ -axis and  $z$ -axis. Overall, the periodic motion law of the primary vibration device with high frequency and low amplitude is verified, making the overall operation of the conveyor separation stable; at the same time, from the high-speed photography attitude tracking trajectory, it can be seen that the movement trajectory of the soil on the conveyor fluctuates less, presenting a microwave shape. There is less interference between adjacent soil blocks. The soil blocks maintain a downstream attitude on the conveyor, and the downstream distance is much greater than the reflux distance, which is consistent with the theoretical analysis results. Under this working parameter, there is less collision between the soil on the sieve surface, which can effectively reduce the collision and friction between potato blocks and between blocks and soil, reduce the rate of skin breakage, and reduce linear scratches. Therefore, the optimal speed combination parameters of the three-stage conveyor separation determined by the no-load test can be used for field experiments.

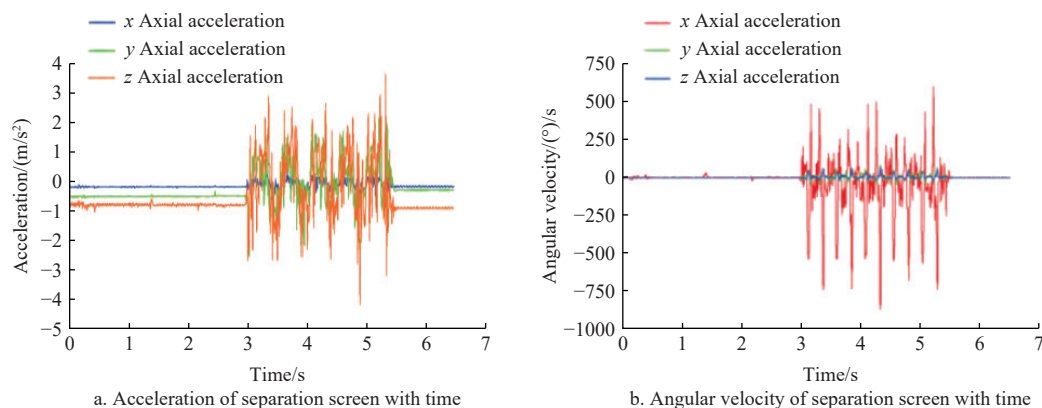


Figure 19 Change of triaxial attitude of separation screen with time

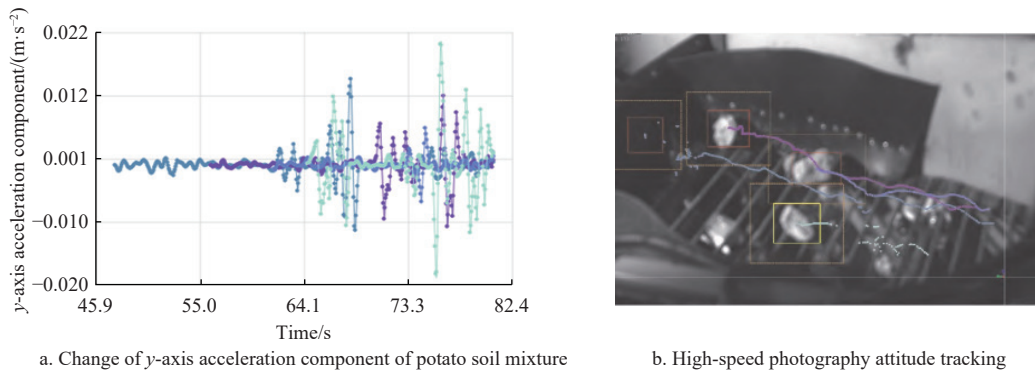


Figure 20 Attitude tracking effect of high-speed photography

**3.2 Effect of field factors on the lifting rate**

The orthogonal test L25 ( $5^4$ ) results in Table 5 illustrate the influence of the four factors with five levels on the lifted potatoes. The highest percentage of lifted potatoes were in treatments ( $W=0.83, D=140, V=III, N=19$ ) and ( $W=1.05, D=180, V=II, N=22$ ), which was 98.8%, while the lowest percentage was in treatment ( $W=1.16, D=180, V=III, N=11$ ), which was 95.8%. The result of this study is better than that from Wang et al.<sup>[6]</sup>, which had a highest lifted potatoes percentage of 96.7% at  $W=1.05$  and  $N=17$ , which was in line with the national standard and met potato harvesting operation requirements.

**Table 5 Results of orthogonal test L25 (54) for various factors**

Test No.	Factors				Test indicators		
	$W/m \cdot s^{-1}$	$D/mm$	$V$	$N(^{\circ})$	Potato lifting/%	Potato damage/%	Potato bruising/%
1	0.75	120	I	7	96.6	0.87	0.69
2	0.75	140	II	11	96.7	0.98	0.85
3	0.75	160	III	15	97.3	1.26	0.94
4	0.75	180	IV	19	98.1	1.69	1.78
5	0.75	200	V	22	98.6	6.97	1.95
6	0.83	120	II	15	97.5	1.64	1.01
7	0.83	140	III	19	98.8	1.73	1.49
8	0.83	160	IV	22	98.6	1.86	1.53
9	0.83	180	V	7	97.4	1.78	1.34
10	0.83	200	I	11	96.1	1.62	1.08
11	0.94	120	III	22	98.6	1.43	1.26
12	0.94	140	IV	7	97.6	1.67	1.59
13	0.94	160	V	11	97.3	2.32	1.76
14	0.94	180	I	15	96.1	1.82	1.54
15	0.94	200	II	19	97.1	1.79	1.68
16	1.05	120	IV	11	95.9	1.35	1.05
17	1.05	140	V	15	97	1.29	1.37
18	1.05	160	I	19	98.1	1.35	0.99
19	1.05	180	II	22	98.8	1.37	1.43
20	1.05	200	III	7	97.4	1.31	1.29
21	1.16	120	V	19	98.7	1.67	1.27
22	1.16	140	I	22	97.8	1.73	1.31
23	1.16	160	II	7	96.6	1.29	1.21
24	1.16	180	III	11	95.8	0.96	0.95
25	1.16	200	IV	15	97.2	0.87	0.64

There was an increase in the lifting of potatoes with a rise in conveyor inclination angle ( $N$ ) L3 and L5, respectively, and a decrease in L2. Pooled data of potato lifting showed that conveyor inclination angle ( $N$ ) L5 had the highest potato lifting with 492.7 kg/experiment, and the most minor potato lifting was

481.8 kg/experiment at conveyor inclination angle ( $N$ ) L2, as shown in Figure 21. Further, it can be seen that the four factors influence the potato lifting rate from high to low, in the order of  $N, V, W,$  and  $D,$  with extreme deviations of 10.9, 4.3, 2.6, and 1.8, respectively. The optimal levels of harvesting operation parameters are: working speed ( $W$ ) of 0.83 m/s, excavation depth ( $D$ ) of 140 mm, vibration intensity ( $V$ ) of Class V, and conveyor inclination angle ( $N$ ) of  $22^{\circ}$ .

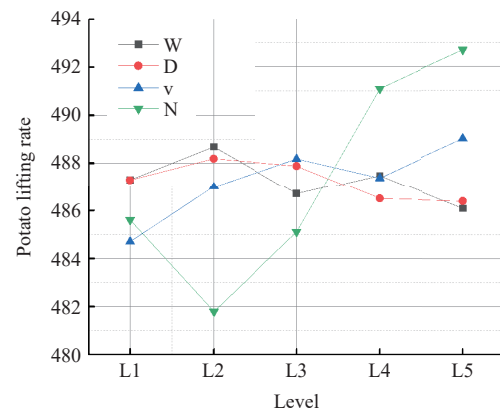


Figure 21 Effect of factors on potato lifting rate

**3.3 Effect of field factors on the damage rate**

The results indicated that the impact of four factors on the potato damage rate ranges from large to small, in the order of  $V, N, D,$  and  $W,$  with extreme deviations of 7.45, 6.41, 5.71, and 5.25, respectively. On the other hand, there was a decrease in the potato damage with a reduction of working speed ( $W$ ) from L1 to L5, where the lowest potato damage was 6.52 kg/experiment at working speed ( $W$ ) L5. In comparison, the highest damage rate was 14.03 kg/experiment at vibration intensity level ( $V$ ) L5, as shown in Figure 22.

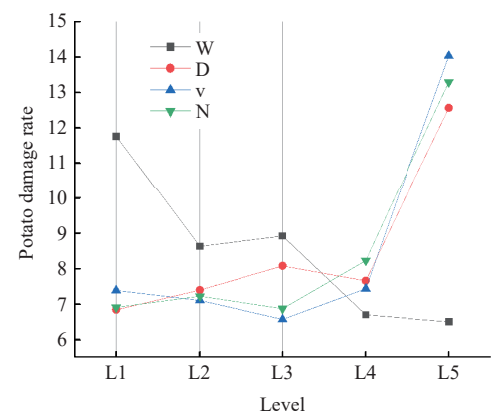


Figure 22 Effect of factors on potato damage rate

The highest percentage of potato damage was 6.97% at treatment ( $W=0.75$ ,  $D=200$ ,  $V=V$ ,  $N=22$ ), while the lowest rate was 0.87% at treatments ( $W=0.75$ ,  $D=120$ ,  $V=I$ ,  $N=7$ ) and ( $W=1.16$ ,  $D=200$ ,  $V=IV$ ,  $N=15$ ), as listed in Table 5. The optimal level of harvesting operation parameters was working speed ( $W$ ) of 1.16 m/s, excavation depth ( $D$ ) of 120 mm, vibration intensity ( $V$ ) of Class III, and conveyor inclination angle ( $N$ ) of 15°, with a damage rate lower than that of 3.36% found in the study by Yang et al.<sup>[52]</sup>, which was 3.36%.

### 3.4 Effect of field factors on the bruising rate

Similarly, the impact of four factors on the rate of bruising potatoes varies as follows, from largest to smallest:  $W$ ,  $V$ ,  $N$ , and  $D$ , with extreme deviations of 2.45, 2.08, 1.65, and 1.87, respectively. The minimum bruising rates were 5.28 and 5.38 kg/experiment at excavation depth ( $D$ ) L<sub>1</sub> and working speed ( $W$ ) L<sub>5</sub>, respectively, while the maximum bruising rates were 7.83 and 7.69 kg/experiment at working speed ( $W$ ) L<sub>3</sub> and vibration intensity level ( $V$ ) L<sub>4</sub>, as shown in Figure 23.

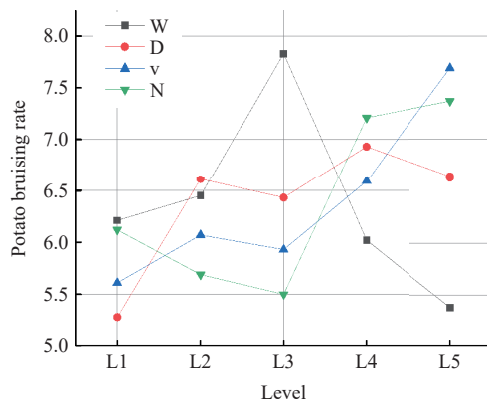


Figure 23 Effect of factors on potato bruising rate

The optimal levels of harvesting operation parameters were: working speed ( $W$ ) of 1.16 m/s, excavation depth ( $D$ ) of 120 mm, vibration intensity ( $V$ ) of Class I, and conveyor inclination angle ( $N$ ) of 15°. The minimum percentage of potato bruising was 0.64% at treatment ( $W=0.75$ ,  $D=120$ ,  $V=I$ ,  $N=7$ ), and the maximum rate was 1.95% at treatment ( $W=0.75$ ,  $D=200$ ,  $V=V$ ,  $N=22$ ), as listed in Table 5.

The values of various experimental factors within a reasonable range and other factors affect the potato harvest. In the operation process, while ensuring the rate of lifting potatoes, it is necessary to strictly meet the standard requirements for the rate of bruising and damaged potatoes. Considering the specific conditions of sticky and compacted soil in Yunnan Province, the operating parameters were comprehensively selected, with a working speed ( $W$ ) of 1.05 m/s, an excavation depth ( $D$ ) of 180 mm, a vibration intensity ( $V$ ) of Class II, and a conveyor inclination angle ( $N$ ) of 22°. The results of the assignment are 98.8% for lifting potatoes, 1.37% for damage, and 1.43% for bruising potatoes, which is better than the results of Ju et al.<sup>[53]</sup> with potato bruising rate of 2.8%. It meets the requirements of national agricultural industry standards.

## 4 Conclusions

1) The potato machine harvester's multi-stage conveying and separating device was designed and tested using SolidWorks software. ANSYS software analyzed the stress, strain, and deformation of the digger's excavation shovel, indicating that the maximum stress value is 47.77 MPa, the maximum strain value is

$2 \times 10^{-4}$  mm, and the maximum deformation is 0.29 mm.

2) The wave-shaped potato soil separation and vibration-crushing methods effectively improved the scattering, crushing, and separation effects of the potato soil mixture and the operating efficiency of the potato harvester in sticky and compacted soil.

3) A no-load test was conducted, and the movement of soil blocks on the conveyor separation was captured and analyzed using a regression model between the influencing factors and the experimental indicators.

4) A no-load test of the conveyor separation indicated that the linear velocity of the primary conveyor separation was ( $Q_3=1.42$  m/s), the linear velocity of the secondary conveyor separation was ( $S_5=2.2$  m/s), the lateral output linear velocity was ( $O_3=1$  m/s), the corresponding soil coverage was 68.96%, and the impurity content was 2.58%.

5) The field orthogonal experiment showed that the optimal working parameters for improving the yield of potatoes were at a working speed of 0.83 m/s, excavation depth of 140 mm, vibration intensity of level V, and conveyor inclination angle of 22°.

6) The optimal working parameters for reducing the potato damage rate were a working speed of 1.16 m/s, an excavation depth of 120 mm, a vibration intensity of level III, and a conveyor inclination angle of 15°.

7) The best parameters to reduce the potato damage rate were a working speed of 1.16 m/s, excavation depth of 120 mm, vibration intensity of level I, and conveyor inclination angle of 15°.

8) Considering the specific situation of sticky and compacted soil in Yunnan Province, a comprehensive selection of a working speed of 1.05 m/s, excavation depth of 180 mm, vibration intensity of level II, and conveyor inclination angle of 22° was made.

9) The total potato rate was 98.8%, the broken skin rate was 1.37%, and the damaged potato rate was 1.43%. All performance results meet the requirements of national industry standards.

## Acknowledgements

This research was funded by the National Key R&D Program Project of Yunnan Provincial Department of Education Science (Grant No. 2022YFD2002004).

## Author Contributions

Conceptualization: Zhaoguo Zhang; Data curation: Ibrahim Issa, Wael El-Kolaly, and Yuan Wang; Formal analysis: Ibrahim Issa and Wael El-Kolaly; Funding acquisition: Zhaoguo Zhang; Methodology: Ibrahim Issa and Wael El-Kolaly; Project administration: Zhaoguo Zhang; Resources: Ibrahim Issa; Software: Ibrahim Issa and Wael El-Kolaly; Supervision: Zhaoguo Zhang and Faan Wang; Validation: Wael El-Kolaly; Writing-original draft: Ibrahim Issa, Wael El-Kolaly, and Yuan Wang; Writing-review & editing: Ibrahim Issa, Wael El-Kolaly, Faan Wang, and Yuan Wang.

## Data Availability

Data were provided by the Faculty of Mechanical and Electrical Engineering and the Faculty of Modern Agricultural Engineering, Kunming University of Science and Technology, for exclusive use in this study and are, in general, not publicly available. Reasonable requests may be addressed to the Faculty of Mechanical and Electrical Engineering and the Faculty of Modern Agricultural Engineering, Kunming University of Science and Technology, China.

## Nomenclature

Symbols	Definitions
$\gamma$	The inclination angle of the shovel blade, ( $^{\circ}$ )
$\varphi$	Friction angle, ( $^{\circ}$ )
$S$	Working width, mm
$M$	Average line spacing, mm
$b$	Average distribution width of potatoes, mm
$\varepsilon$	Comprehensive standard deviation, mm
$c$	Machine line deviation, mm
$\varepsilon_M$	The standard deviation of line spacing, mm
$\varepsilon_b$	The standard deviation of distribution width, mm
$L_1$	Front section length, mm
$L_2$	Rear section length, mm
$h_1$	Average excavation depth, mm
$\delta$	Inclination angle, ( $^{\circ}$ )
$W_f$	Friction work
$W_G$	Gravitational potential energy, J
$R$	Excavator reaction force, N
$t_w$	Movement time shovel surface, s
$m$	Mass of potato soil mixture, kg
$g$	Gravitational acceleration, $m/s^2$
$h_2$	Excavation depth of the rear section, mm
$v_w$	Movement speed, m/s
$F_{N1}$	Reaction force, N
$F_{s1}$	Frictional force, N
$F_{g1}$	Inertial force, N
$m_1$	Mass of the potato soil mixture, kg
$\alpha_1$	Angle surface, ( $^{\circ}$ )
$a$	Acceleration surface, $m/s^2$
$F_{N3}$	Reaction force, N
$F_{s3}$	Frictional force, N
$F_{g3}$	Inertial force, N
$m_3$	Mass of the potato soil mixture, kg
$\alpha_2$	Inclination angle, ( $^{\circ}$ )
$m_4$	Mass of the potato block, kg
$v_0$	Linear velocity, m/s
$h_0$	Height maximum, mm
$h_v$	Vertical height, mm
$t$	Time, s
$x$	Horizontal displacement, mm
$v_{ly}$	Vertical velocity, m/s
$v_{lx}$	Horizontal velocity, m/s
$v_l$	Collision velocity, m/s
$\eta$	Soil coverage on separation sieve, %
$w$	Number of pixels in the separation screen image
$w_i$	Number of pixels in the $i$ -th soil block
$W_1$	The total mass of digging potato, g
$W_2$	The total mass of un-dug potato, g
$W_3$	The total mass of good potato, g
$W_4$	The total mass of potato damaged by the potato harvester, g
$W_5$	The total mass of bruised potatoes, g

## [References]

- [1] Darooghegi M M, Milajerdi A, Sheikhi A, Azadbakht L. Potato consumption and risk of all cause, cancer and cardiovascular mortality: a systematic review and dose-response meta-analysis of prospective cohort studies. *Critical Reviews in Food Science and Nutrition*, 2020; 60(7): 1063–1076.
- [2] Tian J H, Chen J C, Ye X Q, Chen S G. Health benefits of the potato affected by domestic cooking: A review. *Food Chemistry*, 2016; 202: 165–175.
- [3] Wei Z C, Li H W, Sun C Z, Li X Q, Liu W Z, Su G L, et al. Improvement of potato harvester with two segment of vibration and wave separation Transactions of the CSAE, 2018; 34(12): 42–52. DOI: [10.11975/j.issn.1002-6819.2018.12.006](https://doi.org/10.11975/j.issn.1002-6819.2018.12.006). (in Chinese)
- [4] Wei Z C, Li H W, Su G L, Sun C, Liu W, Li X. Development of potato harvester with buffer type potato-impurity separation sieve. *Transactions of the CSAE*, 2019; 35(8): 1–11.
- [5] Kang H B, Liu M, Wang L, Wei M Y, Liu J C, Zhou J D, et al. Simulation analysis of separating and conveying device of potato harvester based on EDEM. *Journal of Agricultural Mechanization Research*, 2022; 44(5): 1–8, 16.
- [6] Wang H Y, Zhang Z G, Ibrahim I, Xie K T, El-Kolaly W, et al. Design and experiment of small-sized potato harvester suitable for hilly and mountainous areas. *Acta Agriculturae Zhejiangensis*, 2021; 33(4): 724–738. DOI: [10.3969/j.issn.1004-1524.2021.04.18](https://doi.org/10.3969/j.issn.1004-1524.2021.04.18).
- [7] Xin L L, Liang J H. Design of conveyor separation device for potato harvester and analysis of its vibration characteristics. *Journal of Computational Methods in Sciences and Engineering*, 2022; 22(4): 1385–1392.
- [8] He X, Li L F, Liu X, Xiao Y M, Jiao T W, Li W. Design and test of potato conveying and grading device with variable space. *Inmatech Agricultural Engineering*, 2023; 69(1): 681.
- [9] Zhang J. China's potato planting area has reached 7000 million mu, and the main producing areas in the west account for more than eighty percent. Available at: <http://www.chinanews.com.cn/cj/2021/10-11/9583694.shtml>.
- [10] Xie S S, Lu K L, Deng W G, Wang F, Li P, Liu G Y. Improved design and experiment of separating sieve for potato digger. *Revista Brasileira de Engenharia Agrícola e Ambiental*, 2023; 27: 966–972
- [11] Ning Q W, Hu L M. China Agriculture Yearbook. Editorial Board of China Agriculture Yearbook, China, 2019.
- [12] Shen X S, Ren D H, Liu X T, Wang P, Qu H J. Current situation, problems and suggestions of potato planting mechanization in Southwest China. *Tillage and Cultivation*, 2018; 1: 41–43.
- [13] Tofeq O M M. Study of the effect of potato lifter line on some properties at different depths and varieties of potato crop. *Acta Technologica Agriculturae*, 2023; 26(2): 108–114.
- [14] Zhang Y S, Hu L R. Yun Nan Statistical Yearbook. China Statistics Press, 2018; ISBN 978-75037-8518-4. (in Chinese)
- [15] Issa I I M, Zhang Z G, El-Kolaly W, Yang X, Wang H Y. Design, ansys analysis and performance evaluation of potato digger harvester. *International Agricultural Engineering Journal*, 2020; 29(1): 60–73.
- [16] Zhan X M, Nie H L, Li Y L. Study on mechanized operation system of rapeseed production in suitable for remediation areas. *Journal of Chinese Agricultural Mechanization*, 2019; 40(7): 197–203.
- [17] Li Q, Luo T, Cheng T, Yang S T, She H J, Li J, et al. Evaluation and screening of rapeseed varieties (*Brassica napus* L.) suitable for mechanized harvesting with high yield and quality. *Agronomy*, 2023; 13(3): 795.
- [18] Amiri Z, Asgharipour M R, Campbell D E, Sabaghi M A. Comparison of the sustainability of mechanized and traditional rapeseed production systems using an emergy-based production function: A case study in Lorestan Province, Iran. *Journal of Cleaner Production*, 2020; 258: 120891.
- [19] Song X Q. Study on whole-process mechanized production mode of spring potato in hilly area. Xintai City Modern Agricultural Development Service Center, 2024; 178p.
- [20] Pu J, Elie N, Zhang B J, Zhang Z H, Xiong S, Zhang L, et al. Sustainable potato production: A model of potato production at low latitude plateau in winter, Yunnan Province, China. Preprints, 2022; DOI: [10.20944/preprints202202.0267.v1](https://doi.org/10.20944/preprints202202.0267.v1)
- [21] Aw K C, Huang W D J, De Silva M W R P. Evaluation of climatic vibration testing on plastic waterproof enclosure for electronic equipment using ANSYS® workbench. *Materials & Design*, 2007; 28(9): 2505–2510.
- [22] Kadam D M, Dongre R, Gupta R, Gautam R, Rajak S K. Performance evaluation of tractor drawn root crop harvester for harvesting of potato and ginger crop. *Biological Forum – An International Journal*, 2023; 15(3): 564–570.
- [23] Wang L H, Liu F, Wang Q, Zhou J Q, Fan X Y, Li J R, et al. Design of a spring-finger potato picker and an experimental study of its picking performance. *Agriculture*, 2023; 13(5): 945.
- [24] Lü J Q, Wang P R, Liu Z F, Li Z H, Zou F Y, Yang D Q. Design and experiment of potato harvester potato stem separation equipment. *Transactions of the CSAM*, 2019; 50(6): 100–109.

- [25] Xie S S, Wang C G, Deng W G. Displacement analysis of potato relative to separation sieve and separation sieve performance test. *Journal of Agricultural Science and Technology*, 2019; 21(8): 71–81.
- [26] Deshvena S, Ramteke R T, Solanki S N. Development and performance evaluation of tractor drawn turmeric digger cum separator. *International Journal of Current Microbiology and Applied Sciences*, 2019; 8(2): 1053–1061.
- [27] Sibirev A, Aksenov A, Dorokhov A, Ponomarev A. Comparative study of the force action of harvester work tools on potato tubers. *Research in Agricultural Engineering*, 2019; 65(3): 85–90.
- [28] Zhou J G, Yang S M, Li M Q, Chen Z, Zhou J D, Gao Z N, et al. Design and experiment of a self-propelled crawler-potato harvester for hilly and mountainous areas. *Inmatch-Agricultural Engineering*, 2021; 64(2): 151–158.
- [29] Li Y Y, Hu Z C, Gu F W, Wang B, Fan J L, Yang H G, et al. DEM-MBD coupling simulation and analysis of the working process of soil and tuber separation of a potato combine harvester. *Agronomy*, 2022; 12(8): 1734.
- [30] Wei Z C, Li H W, Su G L, Sun C, Liu W, Li X. Design and experiment of potato harvester using double cushions for low laying separation technology. *Transactions of the CSAM*, 2019; 50(9): 140–152.
- [31] Sedeeq A, Tofeq O M, Al-Slevani S. An Investigation into the effect of using different harvesting methods on the indicators of potato crop loss. *Mesopotamia Journal of Agriculture*, 2022; 50(3): 19.0–26.0.
- [32] Sang Y Y, Zhang D X, Zhang M M. Study on bruising damage experiment of potato and finite element analysis. *Journal of China Agricultural University*, 2008; 13(1): 81–84.
- [33] Feng B, Sun W, Sun B G, Zhang T, Wu J, Shi L. A study on dropping impact characteristics and damage regularity of potato tubers during harvest. *J. Vib. Shock*, 2019; 38(24): 267–274.
- [34] Abdulla Z, Sedeeq A, Khorshid F. Effects of forward speeds and blade angles of potato digger on fuel consumption and tuber mechanical damages. *Mesopotamia Journal of Agriculture*, 2022; 50(2): 21–37.
- [35] Gai X Z, Wang F, Xie S S, Gao Z H, Deng W G. Effect of drop treatment on potato tuber damage and kinematic characteristics of the sieve rod. *International Agrophysics*, 2023; 37(4): 377–389.
- [36] Lü J Q, Yang X H, Lü Y N, Li Z H, Li J C, Du C L. Analysis and experiment of potato damage in process of lifting and separating potato excavator. *Transactions of the CSAM*, 2020; 51(1): 103–113.
- [37] Liu Q D, Sun W, Wang Y M, Wang J L, Che X L. Simulation of temperature distribution in double-row potato ridges mulched with plastic film covered with soil. *Int J Agric & Biol Eng*, 2024; 17(4): 185–197.
- [38] Aravind M T, Kumar K P, Sharath V, Nithin B, and Krishna S S. Design and analysis of potato harvester. *International Journal of Mechanical Engineering Research and Technology* 2024; 16(2): 477–486.
- [39] Nasr G E, Rostom M N, Hussein M M, Farrag A E, Morsy M F. Finite element analysis (FEA) for potato crop harvester blade suitable for small holdings. *Bioscience Research*, 2018; 15(3): 2702–2710.
- [40] Feng P B, Wang Y N, Mu Y, Un J B, Kang J H, Na W, et al. Effect of high temperature on potato starch content, amylase activity and yield. *Southwest China Journal of Agricultural Sciences*, 2019; 32(6): 1253–1258.
- [41] Lü J Q, Yi S J, Tao G X, Mao X. Parameter optimization and experiment of splitter sliding-knife opener for potato planter. *Transactions of the CSAE*, 2018; 34(4): 44–54.
- [42] Belay D. Design, construction and performance evaluation of potato harvesters: A review international research. *Journal of Engineering & Technology (IRJET)*, 2021; 8(4): 2747–2771.
- [43] Wei H A, Wang D, Lian W X, Yang X P, Huang X P. Development of 4UFD-1400 type potato combine harvester. *Transactions of the CSAE*, 2013; 29(1): 11–17. (in Chinese)
- [44] Du X Q, Li D W, He L Y, Wu C Y, Lin L P. Fruit motion analysis in process of mechanical vibration harvesting based on electronic fruit technique *Transactions of the CSAE*, 2017; 33(17): 58–64. DOI: [10.11975/j.issn.1002-6819.2017.17.008](https://doi.org/10.11975/j.issn.1002-6819.2017.17.008). (in Chinese)
- [45] Tikuneh D B, Bedie A F, Awoke B G. Design, manufacture, and performance evaluation of a single-axle tractor-operated potato digger elevator. *Cogent Engineering*, 2023; 10(2): 2251744.
- [46] Zhao P, Guo R J, Jin T C, Zhang G Z, Ning X F. Collision simulation of potato tubers for mechanized harvesting. *Journal of Food Process Engineering*, 2023; 46(3): e14278.
- [47] Lü J Q, Sun H, Dui H, Peng M M, Yu J Y. Design and experiment on conveyor separation device of potato digger under heavy soil condition. *Transactions of the CSAM*, 2017; 48(11): 146–155.
- [48] Shen H Y, Wang B, Hu L L, Wang G P, Ji L L, Shen G W, Wu T. Design of potato connecting and conveying mechanism for 4UZL-1 type sweet potato combine harvester. *Transactions of the CSAE*, 2020; 36(17): 9–17. [10.11975/j.issn.1002-6819.2020.17.002](https://doi.org/10.11975/j.issn.1002-6819.2020.17.002). (in Chinese)
- [49] Lü J Q, Tian Z E, Wu J e, Yang Y, Shang Q G, Wang Y B, et al. Design and experiment on 4U1Z vibrating potato digger. *Transactions of the CSAE*, 2015; 31(12): 39–47.
- [50] Gu Z J, Zeng Z Y, Shi X Z, Yu D S, Zheng W, Zhang Z L, et al. Estimating models of vegetation fractional coverage based on remote sensing images at different radiometric correction levels. *Frontiers of Forestry in China*, 2009; 4(4): 402–408.
- [51] Xiao F J, Liu Q F, Li S, Qin Y, Huang D P, Wang Y J, et al. A study of the method for retrieving the vegetation index from FY-3D MERSI-II data. *Remote Sensing*, 2023; 15(2): 491.
- [52] Yang X P, Wei H A, Zhao W Y, Jiang Y W, Dai L X, Huang X P. Design and experiment of 4U-1600 set of pile type potato digger. *Transactions of the CSAM*, 2020; 51(6): 83–92.
- [53] Ju Y J, Sun W, Zhao Z W, Wang H C, Liu X L, Zhang H, et al. Development and testing of a self-propelled machine for combined potato harvesting and residual plastic film retrieval. *Machines*, 2023; 11(4): 432.